7.

Cerebral perfusion and glucose metabolism in Alzheimer's disease and frontotemporal dementia: two sides of the same coin?

Sander C.J. Verfaillie, Sofie M. Adriaanse, Maja A.A. Binnewijzend, Marije R. Benedictus, Rik Ossenkoppele, Mike P. Wattjes, Yolande A.L. Pijnenburg,Wiesje M. van der Flier, Adriaan A. Lammertsma, Joost P.A. Kuijer, Ronald Boellaard, Philip Scheltens, Bart N.M. van Berckel and Frederik Barkhof

Under review.

Abstract

Purpose [^{18}F]-2-fluoro-2-deoxy-D-glucose (FDG) positron emission tomography can be used to differentiate between Alzheimer's disease (AD) and frontotemporal (FTD) dementia. Cerebral blood flow (CBF), measured using arterial spin labeling (ASL), is a marker related to metabolism. The aim of this study was to compare ASL and FDG in FTD and AD.

Methods FDG standardized uptake values and ASL derived normalized CBF were measured in 18 AD patients (64±8), 12 behavioral variant FTD patients (age, 61±8), and 10 controls (age, 56±10). Voxel-wise whole-brain comparisons, region of interest (ROI) analysis, Pearson correlation, logistic regression and ROC curves were performed.

Results Age- and sex-adjusted analyses showed decreased CBF and FDG uptake in AD compared with controls and FTD in both precuneus and inferior parietal lobule (IPL) (all p<0.001). Compared with controls and AD, FTD patients showed both hypometabolism and hypoperfusion in the medial prefrontal cortex (mPFC) and orbitofrontal cortex (p<0.001). ROI analyses showed that ASL and FDG were related in precuneus (r=0.62, p<0.001), IPL (r=0.61, p<0.001) and mPFC across groups (r=0.74, p<001). ROC analyses indicated comparable performance of perfusion and metabolism in the precuneus (AUC: 0.72 and 0.74), IPL (0.85 and 0.94) for AD relative to FTD, and in the mPFC in FTD relative to AD (both 0.68).

Conclusion Similar patterns of hypoperfusion and hypometabolism were observed in regions typically associated with AD and FTD pathology, suggesting that ASL provides comparable information as FDG. This study illustrates the potential diagnostic value of ASL in memory clinics.

Introduction

Alzheimer's disease (AD) and frontotemporal dementia (FTD) are among the most common dementias and both are characterized by progressive impairment of cognitive, behavioral and daily functioning [1,2]. Particularly early in the course of the disease, clinical presentation of FTD and AD may overlap or may be misdiagnosed as another psychiatric or neurological disorder. Brain glucose metabolism measured using [^{18}F]-2-fluoro-2-deoxy-D-glucose (FDG) positron emission tomography (PET), provides important additional diagnostic information about brain functioning [3]. Glucose metabolism reflects neuronal (dys)function, which is thought to be an early marker of dementia, preceding structural magnetic resonance imaging (MRI) findings such as cortical atrophy and clinical symptoms [4]. Bilateral temporal-parietal, precuneus and posterior cingulate cortical (PCC) glucose hypometabolism is present in patients with AD, even in a prodromal phase [5-7]. In contrast, FTD patients show marked hypometabolism in the prefrontal cortex and basal ganglia, as well as in the temporal and anterior cingulate cortex (ACC) [8-10]. Based on those findings, FDG improves accuracy in distinguishing between AD and FTD[3,7,11], with high specificity [12,13].

Disadvantages of PET are radiation exposure and relatively high costs. A potential alternative to FDG-PET is the assessment of cerebral blood flow (CBF) measured by perfusion MRI, as CBF is thought to be closely related to metabolism. CBF can be measured non-invasively using arterial spin labeling (ASL). ASL makes use of magnetically labeled water in the arterial blood supply as an endogenous tracer [14,15]. Indeed, comparison of CBF measured with ASL and single photon emission computed tomography provided almost equivalent diagnostic information in AD [16]. For these reasons, ASL might be suitable to identify unique disease-related patterns, just like FDG.

Advantages of ASL are its relatively short acquisition time, low costs, lack of radiation exposure and non-invasiveness, so that ASL can easily be incorporated into standard MRI protocols. In AD patients, ASL studies showed lower CBF in parietal, temporal regions, and PCC [17-20], very similar to FDG findings. In FTD, lower CBF has been found in right frontal regions, and a reduced CBF was found in temporal-parietal and PCC in FTD compared to AD [21,22].

The first study directly comparing FDG and ASL in AD patients and healthy subjects showed corresponding deficits primarily in the angular gyrus and PCC [23]. In addition, visual ratings of both ASL and FDG scans showed excellent distinction between healthy volunteers and AD patients [24]. As such, ASL may have potential clinical use in the diagnostic work-up of dementia. While ASL sequences could be available in nearly every hospital equipped with MRI, perfusion maps are not yet commonly used for diagnostic decision making. ASL, however, is also is a relatively new technique that needs further validation against the more established FDG method in a memory clinic setting. Before it can serve as a more solid biomarker for differential diagnosis in single-subjects, several dementia types have to be firstly compared on group level, and to FDG imaging. To date, no study has compared ASL with FDG in FTD, or compared FTD with AD together with its discriminative performance. Using a retrospective design it allows us to investigate brain function in patients with mild disease state, while ensuring a maintained clinical diagnosis

after approximately two years. Therefore, as further proof-of-concept, the aim of this study was to compare FDG (metabolism) and ASL (perfusion) imaging in the same subjects. More importantly, to what extent aberant brain function, especially in key regions related to dementia, is overlapping between imaging techniques.

Methods

Subjects

A convenience sample consisting of 18 patients with AD, 12 patients with behavioral variant FTD, and 10 controls with available FDG and ASL scans from the Amsterdam Dementia Cohort were included [25]. Subjects were eligible if the interval between FDG and ASL scans did not exceed six months. All patients visited the VU University Medical Center outpatient memory clinic between October 2010 and October 2012. All patients underwent standardized dementia screening: medical history, neuropsychological assessment, physical and neurological examinations, laboratory testing and a structural brain MRI. Clinical diagnosis was established by consensus of a multidisciplinary team, prior to the PET scan, and without the knowledge of the ASL data.

AD patients fulfilled the National Institute of Neurological and Communicative Disorders and Stroke-Alzheimer Disease and Related Disorders Association criteria for probable AD [26]. Alzheimer pathology was verified in all AD patients using parametric non-displaceable bindings potential images based on 90-minute dynamic Pittsburgh Compound-B (PIB) PET scans.

All FTD patients met the criteria for probable behavioral variant FTD.[27] All AD and FTD patients were eligible if this diagnosis was maintained after a clinical follow-up period of at least one year. Controls were patients with subjective memory complaints that lacked verified cognitive disorders or any relevant psychiatric disorders, and who showed no evidence of a neurodegenerative disorder on MRI [18]. In addition, controls were selected to have normal CSF Aß1-42 levels, to exclude possible preclinical AD cases.

The study was approved by the Medical Ethics Review Committee, and all subjects provided written informed consent.

PET

Fifteen minutes prior to injection patients were instructed to rest with eyes closed and earplugs in a dimly lit room with minimal background noise. Patients underwent a 15 minutes emission scan (3x5 minutes frames), 45 minutes after intravenous bolus injection of 188±8 MBq [^{18}F]FDG. FDG emission scans were obtained using a Gemini TF 64 PET-CT (Philips Medical Systems, Cleveland, Ohio, US) or ECAT HR+

(Siemens/CTI, Knoxville, US) scanner (respectively AD, n=6/ n=12; FTD, n=7/ n=5; controls n=3/ n=7). Details about scan acquisition have been described elsewhere [28]. All PET unreconstructed data (sinograms) were normalized, and corrected for randoms, dead time, scatter and decay. Attenuation correction was performed using a low-dose CT (PET-CT) or transmission scan (ECAT HR+). The reconstruction protocol has been described elsewhere [29], but included standard reconstruction algorithms for both scanners (ECAT HR+: standard filtered back-projection; PET-CT 3D row-action maximum likelihood algorithm). Finally, standardized uptake values (SUV) were calculated, normalized for injected dose, body weight and length, using in-house developed software and procedures [30]. SUV images were normalized to global uptake using SPM8 (Statistical Parametric Mapping; Wellcome Trust Center for Neuroimaging, London, UK).

MRI

MRI scans were acquired on a 3T whole body MR system (SignaHDxt, GE Medical Systems Milwaukee, WI, USA) using an 8-channel head coil. The MRI acquisition protocol has extensively been described elsewhere [18] and included a sagittal 3D T1-weighted inversion recovery fast spoiled gradient echo. ASL-MRI sequence was provided by GE. Pseudo-continuous ASL perfusion images (3D fast-spin echo acquisition with background suppression, post-label delay 2.0s, TR = 4.8s, TE = 9ms, spiral readout 8 arms x 512 samples; 36x5.0 mm axial slices, 3.2x3.2 mm^2 in-plane resolution, reconstructed pixel size 1.7x1.7 mm^2, acquisition time 4 minutes) were calculated after subtraction of labeled from control images. Both T1-weighted and ASL images were corrected for gradient non-linearity in all three directions. Perfusion was normalized to global perfusion using SPM8, just like FDG.

Image analysis

Preprocessing and between group image comparisons were performed using SPM8 in Matlab (MathWorks, Release 2010a). Parametric images of FDG-SUV and ASL derived CBF were co-registered to the structural T1 image, and spatially registered to Montreal Neurological Institute (MNI) space (voxel size: 2.0x2.0x2.0 mm^3) [31]. ASL images were spatially smoothed using an 8mm full-width at half-maximum Gaussian kernel, corresponding to the smoothing kernel of FDG images at reconstruction. Group effects were investigated separately for ASL and FDG with a voxel-wise contrast including covariates (age and sex), to adjust for common confounding effects [32]. To reliably and validly compare normalized signals of both techniques in grey matter, proportional scaling, mean global calculation and grey matter masking was applied in SPM8. Because we were interested in the concordance of spatial abnormality patterns and corresponding standard normal deviate relative to controls, SPM derived mean *Z*-scores were extracted from multiple significant clusters (thresholded at $p<0.001$ uncorrected for multiple comparisons (cluster size ≥10)).

To investigate to what extent FDG and ASL correlate, region of interest (ROIs) analysis

were performed. Based on the most significant clusters derived from patients versus controls comparisons that (partially) overlapped between FDG and ASL, post-hoc ROI analysis was done using MarsBaR (v0.43, Marseille, France). Functional ROIs encompassed both FDG and ASL regional abnormal clusters at liberal threshold (defined through SPM local maxima $p<0.05$ uncorrected), ensuring a large enough target region.

In total 3 separate ROIs were created for AD (n=2) and FTD (n=1) signature regions (supplementary figures). ROIs coordinates AD: precuneus (xyz ASL -10/-68/30, FDG -2/-70/32) and inferior parietal lobule (IPL) (xyz ASL 44/-56/46, FDG 46/-58/40). ROI coordinates FTD: mPFC (xyz ASL 2/62/6, FDG 6/60/6). Next, a combined (ASL+FDG) signature ROI was saved as a single cluster, and trimmed with a box (20x20x20 mm^3) at intermediate voxel coordinates (precuneus: -6/-69/31, IPL: 45/-57/43, mPFC: 4/61/6). Trimming was done to remove extraneous voxels (i.e. outside signature region). ROI values were extracted with default settings.

Statistical analysis

Demographic and clinical data were analyzed using the Statistical Package for Social Sciences (SPSS) version 20.0.0 (IBM Corp., Armonk New York, U.S.). If data deviated from normality (using Kolmogorov-Smirnov tests for non-normality), non-parametric tests were used, as indicated. Demographic (age, body weight and length) and MMSE were assessed using ANOVA. Gender differences were assessed using χ^2 tests. Across groups, the relationship between FDG and ASL was investigated using Pearson correlation.

Across group (AD, FTD, controls) comparative performance was investigated using binary logistic regression with all FDG and ASL ROI values entered simultaneously as input, and dummy coded dementia group as dependent variable. Multicollinearity assumptions were investigated using linear regression methods. Further, to investigate to what extent FDG and ASL is able to discriminate between AD and FTD, receiver operating characteristic (ROC) curves were generated to obtain an area under the curve (AUC). Specifically, ASL and FDG separate ROI values from AD and FTD patients were used as input (test variable), dementia group was set as state variable. In addition, mean difference scores of signature ROIs were calculated to investigate if subtracting signature regions would result better discriminative performance.

Results

Demographic and clinical variables are presented in Table 1. Age, gender, time intervals and FDG SUV normalization variables (body weight and length, injected dose) did not differ between groups. The frequency distribution of PET scanners (PET-CT and HR+) was not different between groups ($\chi^2(2) = 1.6$, $p=0.21$). The combined dementia groups showed lower MMSE scores ($F(38,1) = 1.8$, $p=0.01$) than controls,

but did not differ between each other. All amyloid PET scans of the AD patient group were classified as being consistent with abnormal amyloid load. All FTD patients had normal cerebrospinal fluid (CSF) Aß1-42 levels (n=3) or negative amyloid PET scan (n=8). In one FTD patient amyloid-specific information was missing. Figure 1 shows raw ASL and FDG images with corresponding MRI of a typical AD and FTD patient.

Figure 1. Transversal FDG and ASL images of an FTD (first and second row, MMSE 26, female 53 years old) and an AD (third and fourth row, MMSE 17, female 52 years old) patient. Both transversal planes show predominant prefrontal abnormalities in FTD and parietal abnormalities in AD. 'Red color' reflects normal metabolism and perfusion.

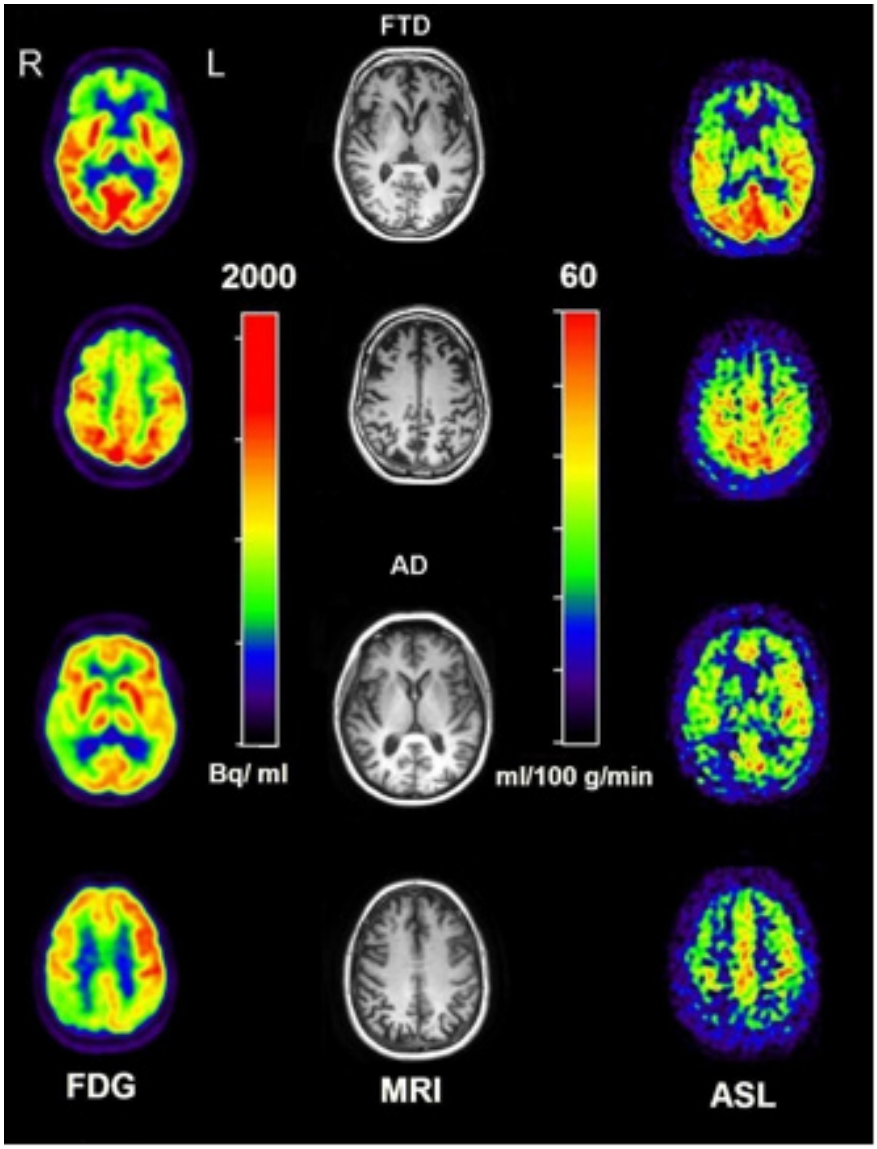

Table 1: Demographic and clinical data

Patient group Characteristics	AD N=18	FTD N=12	CONTROLS N=10	Test-statistic (p-value)
Age in years (SD)	64 (8)	61 (8)	56 (10)	$F(37,2)=1.9$, p=0.17
Gender (% male)	61%	42%	90%	$\chi 2(2)=5.5$, p=0.06
MMSE (SD)	24 (4)	24 (4)	27 (3)	$F(37,2)=2.6$, p=0.09
Scan interval in months (SD)	2.1 (1)	2.2 (2)	1.9 (2)	$F(37,2)=.8$, p=0.5
FDG SUV normalization variables				
Body -weight in kg (SD) -length in cm (SD)	78 (11) 176 (9)	75 (15) 169 (10)	86 (17) 175 (9)	$F(37,2)=2.2$, p=0.13 $F(37,2)=1.5$, p=0.23
Injected Dose in MBq (SD)	190 (8)	187 (8)	188 (7)	$F(37,2)=.97$, p=0.39

Figure 2 shows regional abnormalities derived from groups comparisons projected onto a MNI glass brain, whereas figure 3A shows Z-scores FTD and AD compared to controls (MNI coordinates and cluster sizes can be found in the supplementary data). Compared with controls, in AD both lower metabolism (FDG) and lower perfusion (ASL) was found in bilateral precuneus, bilateral inferior parietal lobule (IPL) and dorsolateral prefrontal cortex (DLPFC). In addition, AD patients showed lower perfusion in orbitofrontal cortex (OFC). Compared with controls, FTD patients showed both lower metabolism and perfusion in mPFC, OFC and temporal poles. In addition, hypoperfusion was found in the supplementary motor area (SMA), and hypometabolism in the DLPFC in FTD. Overall, mean Z-score range (reflecting normal deviate) was comparable between ASL and FDG in patient relative to controls.

Compared with FTD, AD patients showed lower metabolism in precuneus and bilateral IPL, whereas lower perfusion was observed in precuneus and left IPL (figure 3B). In addition, lower perfusion was found in the middle temporal gyrus (MTG) in AD than in FTD, with the opposite pattern in SMA, OFC, temporal poles and mPFC. Likewise, lower metabolism was found in OFC, SMA, mPFC, temporal poles, and anterior PFC (aPFC) in FTD relative to AD. While, OFC hypometabolism was located in anteromedial orbitofrontal parts, hypoperfusion was predominantly found in posterolateral parts extending to temporal poles.

Correlations between regional FDG and ASL values are shown in Figure 4. Across groups a strong correlation between FDG and ASL was found in mPFC (Fig 4A. r= .74, p< 0.001), IPL (Fig 4B. r= .61, p<0.001) and precuneus (r= .62, p<0.001).

The predictive value of all groups' (AD, FTD, controls) separate ROIs ((IPL, precuneus, mPFC) x FDG& ASL) was investigated for AD and FTD using logistic regression. There was a significant fit of the data in AD ($\chi^2(6)$ =44.1, p<0.001), predicted by IPL metabolism (β±S.E. 0.54±0.31, p=0.046), but not by IPL (β±S.E. 0.71±0.31) or precuneus (β±S.E. 0.88±0.12) perfusion, or precuneus (β±S.E. 0.94±0.1113) metabolism. To exclude significant multicollinearity, testing was done and showed no violations (all variables: Tolerance >0.41, VIF<2.46). In contrast for FTD, there was a significant fit of the data ($\chi^2(6)$ =32.1, p<0.001), predicted mPFC perfusion (β±S.E. 0.74±0.16, p=0.026), but not mPFC (β±S.E. 0.89±0.15) metabolism. Multicollinearity testing showed no violations (all variables: Tolerance >0.40, VIF<2.52).

Figure 2. Functional brain abnormalities of AD and FTD compared to controls projected onto a MNI glass brain. Predominant parietal, precuneus aberrant function is visible in AD compared to controls, while FTD compared to controls shows mostly prefrontal abnormalities with FDG as well as ASL. For illustrative purposes, images were thresholded at p<0.005.

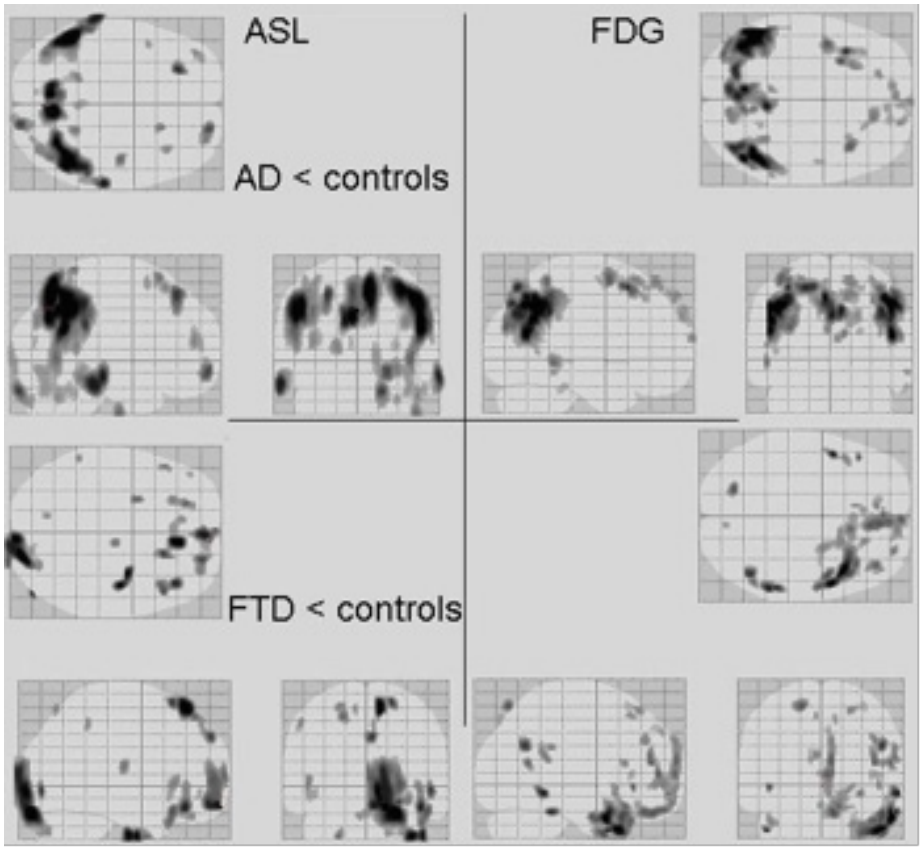

Figure 3. Panel A shows FDG and ASL regional mean Z-scores of AD (left) and FTD (right) compared to controls. Panel B shows AD < FTD (left) and FTD < AD (right) perfusion and metabolism abnormalities.

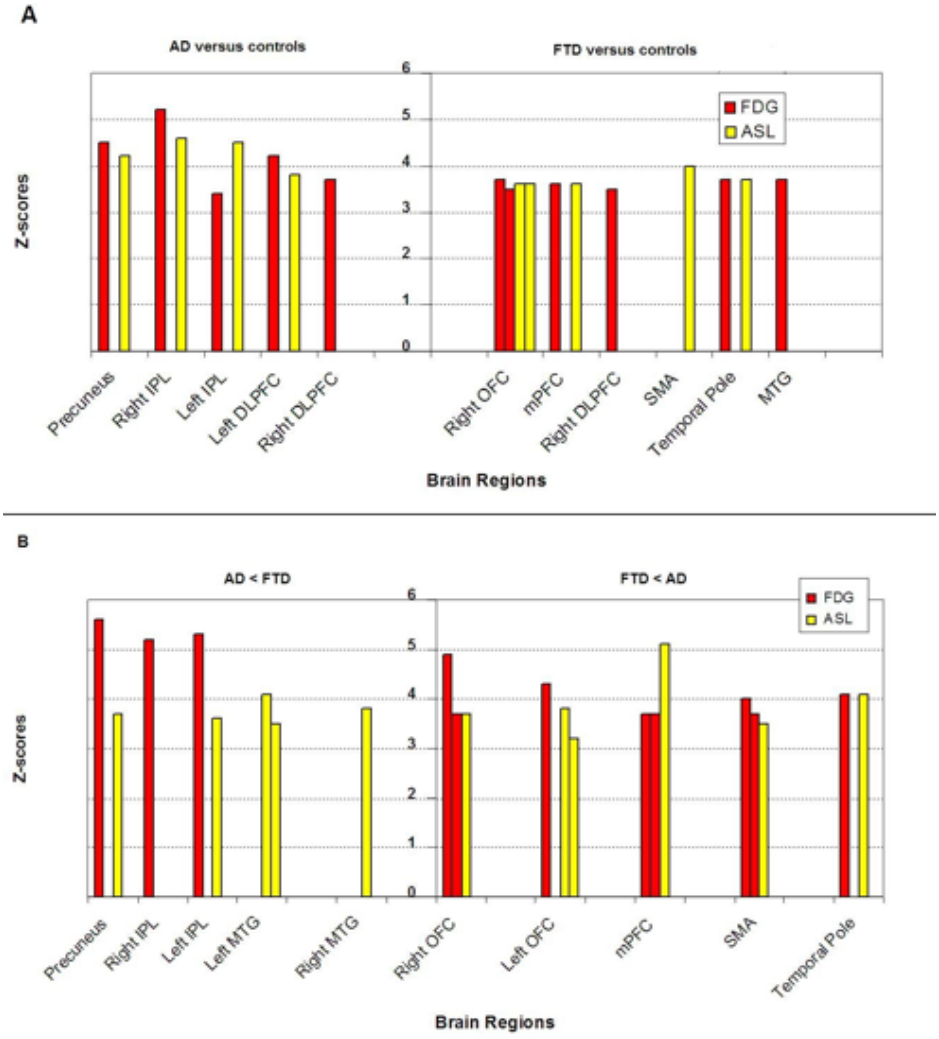

To investigate the discriminative power of ASL and FDG for AD and FTD, ROC curves were generated. Figure 5 shows ROC curves for AD and FTD based on precuneus (Figure 5A) and mPFC (Figure 5B) ROI values. Precuneus AUC was 0.74 for FDG and 0.72 for ASL. For IPL, AUC was 0.94 for FDG and 0.85 for ASL. For mPFC, AUC was 0.68 for both FDG and ASL. Additionally, ratios (between mPFC and precuneus, and mPFC and IPL) were used for discriminating AD from FTD, these showed for precuneus AUC values of 0.80 and 0.90, and for IPL 0.89 and 0.96 for FDG and ASL, respectively. Likewise, for discriminating FTD from AD, mPFC showed an AUC of 0.82 for FDG and 0.89 for ASL.

Figure 4. Positive correlations between FDG SUV and ASL derived CBF in (4b) inferior parietal lobule (left, r = .61, p<.001) and (4a) medial prefrontal cortex (right, r = .74, p< .001) across groups.

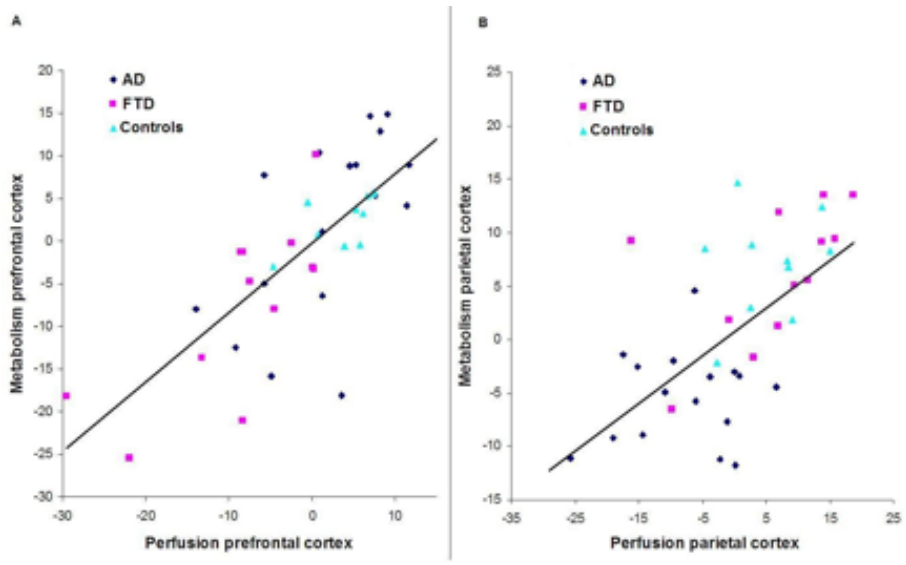

Figure 5. ROC curves for FDG and ASL in AD and FTD. 5A shows precuneus function for ASL and FDG in discriminating AD from FTD. 5B shows mPFC function in discriminating FTD from AD. Ratios were taken between the mPFC and precuneus and entered into ROC analyses as 'ratio ROI'.

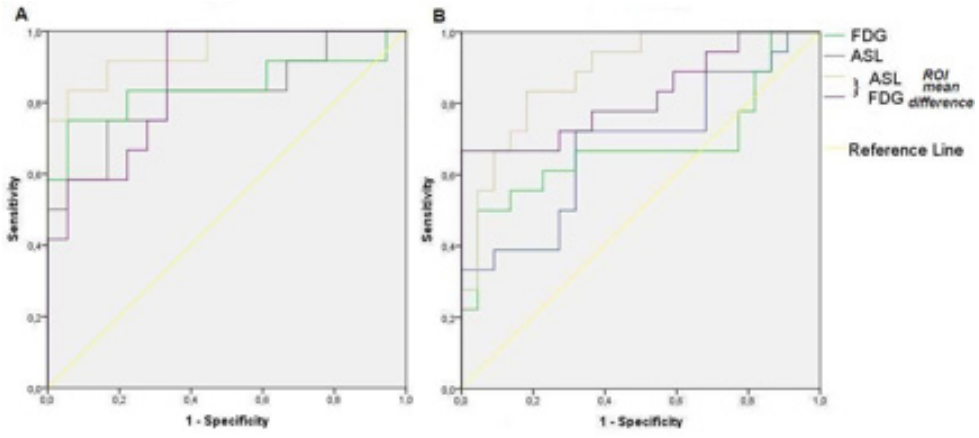

Discussion

In this study, FDG and ASL were compared in AD and FTD patients. The main finding of this study is that glucose metabolism and perfusion show similar spatial abnormalities in both AD and FTD as compared with cognitively normal subjects, in areas consistent with disease models. Overall, these findings emphasize the role of ASL for assessing spatial patterns of aberrant brain function in dementia. This suggests a potential use in memory clinics.

So far, quantitative and qualitative FDG studies consistently have demonstrated glucose hypometabolism in bilateral temporal-parietal, precuneal regions in AD [5-7], which are associated with neuropsychological deficits [35] and structural MRI atrophy [36]. The present FDG results on AD are in line with previous reports, indicating severely abnormal metabolism especially in bilateral IPL.

The present study also demonstrated ASL hypoperfusion in bilateral IPL in AD compared with controls, in line with a previous study using voxel-wise analyses [20]. In another study unilateral IPL hypoperfusion was seen [19], which might be due to a globally decreased perfusion [18]. Furthermore, in AD compared with controls, hypoperfusion was also observed in bilateral precuneus. In short, these results are in line with voxel-wise ASL studies reporting decreased CBF in PCC and parietal cortex in AD compared with controls [17-20].

With regard to FTD, metabolic impairment, often asymmetric, has been reported in frontal, subcortical, ACC and temporal regions [7-9]. The present FDG results are partially in line with these existing reports, as hypometabolism was observed in frontal lobes and temporal poles, but not in basal ganglia. One explanation could be that subcortical metabolic deficits are associated with advanced disease states [9,10] or co-morbid motor-neuron disease [8]. In the present study, however, behavioral variant FTD patients mainly with mild dementia were included.

In FTD compared with controls, functional abnormalities in the frontal lobe were found with ASL, in line with previous studies [21-22]. While some studies demonstrated bilateral [22] and right [21] frontal deficits, the present findings point to predominant dorsomedial prefrontal hypoperfusion. Nevertheless, multiple regions in the frontal lobe are associated with the behavioral phenotype [37].

Taken together, similar functional deficits were found in AD and FTD with both FDG and ASL, and these deficits are consistent with well-known pathophysiological disease models [4,27,37]. Both imaging techniques showed comparable discriminative performance in terms of AUC. For AD signature ROIs, FDG showed slightly larger AUCs compared to ASL, whereas we found the opposite if the mean difference was taken between AD and FTD ROIs. For AD, IPL showed slightly better differentiation between AD and FTD compared to the precuneus using either FDG or ASL. In addition, regression analyses indicated that IPL metabolism was the strongest predictor for AD if compared to all other ROIs, but ASL prefrontal perfusion in FTD. Nevertheless, regional FDG and ASL values were correlated in the precuneus, IPL, and most clearly in the frontal lobe across groups. In contrast, voxel-wise abnormalities were most comparable in AD compared to controls, and to a lesser extent in FTD. This might

be caused by distinct and broad frontal deficiencies known to be present in FTD. To date, only one study has been reported in which a voxel-wise comparison between ASL and FDG was performed in AD. Chen et al. showed overlapping functional abnormalities in the PCC and angular gyri [23]. The present results endorse those findings, but additionally provide first evidence of largely overlapping functional abnormalities between imaging techniques also in FTD, already with mild disease severity. Current findings further demonstrate that both techniques can comparably discriminate between the two most common early-onset dementia groups.

While overlapping ASL perfusion abnormalities relative to FDG was demonstrated on group level, future studies are necessary to clarify the clinical potential of this application on single subjects, while also controlling for common confounding effects. Furthermore, the capabilities of ASL should be investigated in more complex dementia cases or variants, or even in other neuropsychiatric disorders. Also, to ensure general use, performance should be tested on different MRI scanners. Lastly, for potential clinical use, visualization and assessment of CBF maps could benefit from scientific agreement on smoothing kernels for optimal signal-to-noise ratio.

This study had several potential limitations. Since our aim was to compare imaging techniques performance in such a way that it could be extrapolated to a realistic clinical setting, our data was uncorrected for partial volume effects, which could occur due to cerebral atrophy. We therefore cannot distinguish true decreases in brain tissue perfusion and metabolism from apparent decreases in brain function by increased CSF volume. Nevertheless, there are consistent reports of functional brain abnormalities persisting after partial volume correction in AD and FTD [38,39]. In addition, similar processing pipelines were used for both techniques. In addition, applying these corrections could have introduced unwanted variability in key brain regions. Until now, no ideal partial volume correction methods is available for both methods [40]. Secondly, in all cases, FDG scans were performed roughly two months after MR acquisition. It should be noted that consecutive MRI and PET acquisitions resembles a realistic diagnostic workup. Thirdly, the current study used a convenience sample, consisting of patients with extensive differential diagnosis, which may have biased our results in that clear-cut cases (i.e. FDG scan not necessary) were not included. For this reason not all FTD patients exhibited frontotemporal atrophy on MRI. Notwithstanding, this study did show overlapping aberrant function already in cases with mild disease severity, which renders it suitable for early diagnosis. Fourthly, subjects with cognitive complaints but without any verified abnormalities were used as a reference group. This control group consisted of primarily males. Despite statistically adjusting analyses for gender effects, this might have influenced our results. Liu and colleagues, however, showed that no specific regional hypoperfusion is related to gender effects [32]. For this reason it is likely that our regional abnormalities do reflect dysfunction related to AD and FTD pathology. Another point of debate about our controls is that current knowledge, especially regarding brain function, is limited on this heterogeneous group. On the other hand one could argue that more rigorously defined controls might be 'healthier' than 'normal' elderly, and that our control group reflects clinical practice better. Lastly, many uncontrolled factors like smoking and caffeine intake may have affected measurements to a certain extent.

In conclusion, comparable reduced cerebral perfusion and metabolism were observed

predominantly in parietal cortex and PCC in AD, and in frontal lobes in FTD, in line with pathophysiological disease models. ASL could therefore be considered as a promising adjunct to clinical investigations, even for early diagnosis.

Acknowledgments

Research of the VUmc Alzheimer center is part of the neurodegeneration research program of the Neuroscience Campus Amsterdam. The VUmc Alzheimer center is supported by Alzheimer Nederland and Stichting VUmc fonds. The authors thank Ajit Shankaranarayanan of GE Healthcare for providing the 3D pseudo-continuous ASL sequence that was used to obtain data for this paper.

Supplementary Tables and Figures

Table 2: FDG and ASL voxelwise comparisons between patient groups

Contrast	Brain Region	FDG	ASL
		Brain MNI coordinates (x/y/z) Z-value (number of voxels)	
AD < controls	Precuneus	(-2/-70/32) 4.5 (483)*[b]	(-10/-68/30) 4.2 (1085)*[b]
	IPL	(46/-58/40) 5.2 (816)	(44/-56/46) 4.6 (1401)
		(-46/-56/38) 3.4 (1260)	(-52/-50/38) 4.5 (783)
	DLPFC	(40/16/54) 3.7 (19)	(-26/34/50) 3.8 (65)
		(-36/16/54) 4.2 (21)	
	OFC		(22/58/-12) 3.7 (57)
FTD < controls	mPFC	(6/60/6) 3.6 (36)	(2/62/6) 3.6 (118)
	OFC	(8/44/-24) 3.7 (81)	(24/54/-16) 3.6 (13)
		(12/20/-20) 3.5 (11)	(42/34/-20) 3.6 (24)
	STG	(48/-60/28) 3.9 (32)	
	Temporal pole	(46/18/-32) 3.7 (337)	(34/-6/-42) 3.7 (64)
	DLPFC	(42/42/16) 3.5 (16)	
	SMA		(8/34/58) 4 (96)
	MTG	(58/-32/-23) 3.7 (25)	
AD < FTD	Precuneus	4/-60/38 5.6 (60)	4/-58/44 3.7 (243)
	IPL	-46/-60/38 5.3 (4187)	-42/-56/56 3.6 (57)
		40/-70/40 5.2 (363)	
	MTG		-50/-44/0 4.1 (531)
			56/-42/0 3.8 (296)
			-46/-64/-8 3.5 (81)

FTD < AD	OFC	34/22/-4 4.9 (2519) -40/30/-8 4.3 (83) 18/58/-10 3.7 (21)	-8/34/-22 3.8 (197) -48/20/4 3.2 (19) 52/22/8 3.7 (29)
	mPFC SMA	8/46/28 3.7 (31) 18/58/-10 3.7 (21) (-8/28/50) 4 (40) 12/30/48 3.7 (25)	4/52/0 5.1 (846) 8/32/62 3.5 (67)
	ACC	-8/28/50 4.9 (595)	
	Temporal Pole	-30/16/-30 4.1 (101)	32/24/-34 4.1 (454)

Abbreviations: ACC, anterior cingulate cortex; aPFC, anterior prefrontal cortex; DLPFC, dorsolateral prefrontal cortex; IPL, inferior parietal lobule; mPFC, medial prefrontal cortex; MTG, middle temporal gyrus; OFC, orbitofrontal cortex; PFC, prefrontal cortex; SMA, supplementary motor cortex; STG, superior temporal gyrus; *Precuneus including the posterior cingulate gyrus; b, bilateral . Cluster sizes and MNI coordinates were based on p<.001 uncorrected for multiple comparisons.

Figure 6. Functional region-of-interest (ROI) used for FDG-ASL comparisons. ROIs were based on patient to controls comparisons for each technique (at liberal threshold), then FDG and ASL were merged into one signature ROI, and trimmed with 20x20x20mm box to remove extraneous voxels. The ROIs consist of the following volumes (in mm): mPFC, 3984; precuneus, 8360; IPL 5408.

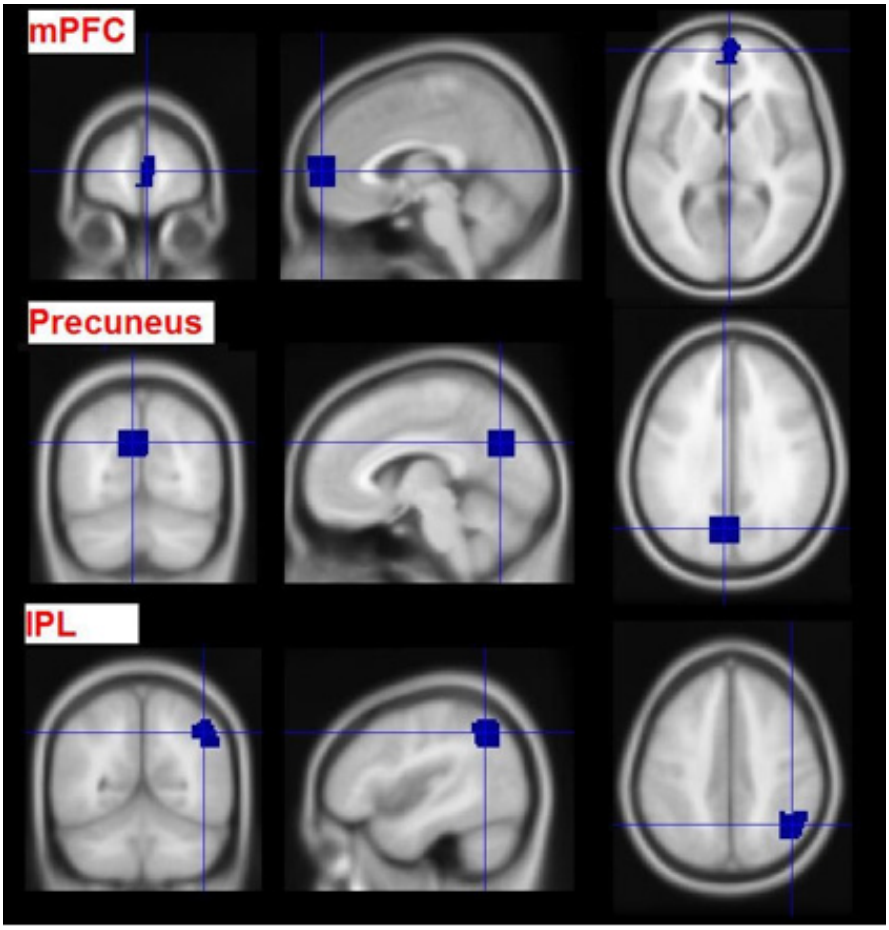

References

[1] Association As. 2012 Alzheimer's disease facts and figures. Alzheimers Dement. 2012;8(2):131-168.

[2] Ratnavalli E, Brayne C, Dawson K, et al. The prevalence of frontotemporal dementia. Neurology. Jun 11 2002;58(11):1615-1621.

[3] Bohnen NI, Djang DS, Herholz K et al. Effectiveness and safety of 18F-FDG PET in the evaluation of dementia: a review of the recent literature. J Nucl Med. Jan 2011;53(1):59-71.

[4] Jack CR, Jr., Knopman DS, Jagust WJ, et al. Tracking pathophysiological processes in Alzheimer's disease: an updated hypothetical model of dynamic biomarkers. Lancet Neurol. Feb 2013;12(2):207-216.

[5] Hoffman JM, Welsh-Bohmer KA, Hanson M, et al. FDG PET imaging in patients with pathologically verified dementia. J Nucl Med. Nov 2000;41(11):1920-1928.

[6] Minoshima S, Giordani B, Berent S, et al. Metabolic reduction in the posterior cingulate cortex in very early Alzheimer's disease. Ann Neurol. Jul 1997;42(1):85-94.

[7] Mosconi L, Tsui WH, Herholz K, et al. Multicenter standardized 18F-FDG PET diagnosis of mild cognitive impairment, Alzheimer's disease, and other dementias. J Nucl Med. Mar 2008;49(3):390-398.

[8] Jeong Y, Cho SS, Park JM, et al. 18F-FDG PET findings in frontotemporal dementia: an SPM analysis of 29 patients. J Nucl Med. Feb 2005;46(2):233-239.

[9] Diehl-Schmid J, Grimmer T, Drzezga A, et al. Decline of cerebral glucose metabolism in frontotemporal dementia: a longitudinal 18F-FDG-PET-study. Neurobiol Aging. Jan 2007;28(1):42-50.

[10] Grimmer T, Diehl J, Drzezga A, Forstl H, et al. Region-specific decline of cerebral glucose metabolism in patients with frontotemporal dementia: a prospective 18F-FDG-PET study. Dement Geriatr Cogn Disord. 2004;18(1):32-36.

[11] Foster NL, Heidebrink JL, Clark CM, et al. FDG-PET improves accuracy in distinguishing frontotemporal dementia and Alzheimer's disease. Brain. Oct 2007;130(Pt 10):2616-2635.

[12] Panegyres PK, Rogers JM, McCarthy M, et al. Fluorodeoxyglucose-positron emission tomography in the differential diagnosis of early-onset dementia: a prospective, community-based study. BMC Neurol. 2009;9:41.

[13] Rabinovici GD, Rosen HJ, Alkalay A, et al. Amyloid vs FDG-PET in the differential diagnosis of AD and FTLD. Neurology. Dec 6 2011;77(23):2034-2042.

[14] Alsop DC, Detre JA. Multisection cerebral blood flow MR imaging with continuous arterial spin labeling. Radiology. Aug 1998;208(2):410-416.

[15] Detre JA, Leigh JS, Williams DS, Koretsky AP. Perfusion imaging. Magn Reson Med. Jan 1992;23(1):37-45.

[16] Takahashi H, Ishii K, Hosokawa C, et al. Clinical Application of 3D Arterial Spin-Labeled Brain Perfusion Imaging for Alzheimer Disease: Comparison with Brain Perfusion SPECT. AJNR Am J Neuroradiol. Nov 21 2013.

[17] Alsop DC, Dai W, Grossman M, Detre JA. Arterial spin labeling blood flow MRI: its role in the early characterization of Alzheimer's disease. J Alzheimers Dis. 2010;20(3):871-880.

[18] Binnewijzend MA, Kuijer JP, Benedictus MR, et al. Cerebral blood flow measured with 3D pseudocontinuous arterial spin-labeling MR imaging in Alzheimer disease and mild cognitive impairment: a marker for disease severity. Radiology. Apr 2012;267(1):221-230.

[19] Dai W, Lopez OL, Carmichael OT, et al. Mild cognitive impairment and alzheimer disease:

patterns of altered cerebral blood flow at MR imaging. Radiology. Mar 2009;250(3):856-866.

[20] Johnson NA, Jahng GH, Weiner MW, et al. Pattern of cerebral hypoperfusion in Alzheimer disease and mild cognitive impairment measured with arterial spin-labeling MR imaging: initial experience. Radiology. Mar 2005;234(3):851-859.

[21] Du AT, Jahng GH, Hayasaka S, et al. Hypoperfusion in frontotemporal dementia and Alzheimer disease by arterial spin labeling MRI. Neurology. Oct 10 2006;67(7):1215-1220.

[22] Hu WT, Wang Z, Lee VM, et al. Distinct cerebral perfusion patterns in FTLD and AD. Neurology. Sep 7 2010;75(10):881-888.

[23] Chen Y, Wolk DA, Reddin JS, et al. Voxel-level comparison of arterial spin-labeled perfusion MRI and FDG-PET in Alzheimer disease. Neurology. Nov 29 2011;77(22):1977-1985.

[24] Musiek ES, Chen Y, Korczykowski M, et al. Direct comparison of fluorodeoxyglucose positron emission tomography and arterial spin labeling magnetic resonance imaging in Alzheimer's disease. Alzheimers Dement. Jan 2012;8(1):51-59.

[25] van der Flier WM, Pijnenburg YA, Prins N, et al. Optimizing patient care and research: the amsterdam dementia cohort. J Alzheimers Dis. 2014;41(1):313-327.

[26] McKhann GM, Knopman DS, Chertkow H, et al. The diagnosis of dementia due to Alzheimer's disease: recommendations from the National Institute on Aging-Alzheimer's Association workgroups on diagnostic guidelines for Alzheimer's disease. Alzheimers Dement. May 2011;7(3):263-269.

[27] Rascovsky K, Hodges JR, Knopman D, et al. Sensitivity of revised diagnostic criteria for the behavioural variant of frontotemporal dementia. Brain. Sep 2011;134(Pt 9):2456-2477.

[28] Ossenkoppele R, Zwan MD, Tolboom N, et al. Amyloid burden and metabolic function in early-onset Alzheimer's disease: parietal lobe involvement. Brain. Jul 2012;135(Pt 7):2115-2125.

[29] Ossenkoppele R, Tolboom N, Foster-Dingley JC, et al. Longitudinal imaging of Alzheimer pathology using [(11)C]PIB, [(18)F]FDDNP and [(18)F]FDG PET. Eur J Nucl Med Mol Imaging. Mar 23 2012.

[30] Boellaard RY, M; Lubberink, M; Lammertsma, A. PPET: a software tool for kinetic and parametric analyses of dynamic PET studies. Neuroimage. 2006 2006;31.

[31] Jenkinson M, Smith S. A global optimisation method for robust affine registration of brain images. Med Image Anal. Jun 2001;5(2):143-156.

[32] Liu Y, Zhu X, Feinberg D, et al. Arterial spin labeling MRI study of age and gender effects on brain perfusion hemodynamics. Magn Reson Med. Sep 2012;68(3):912-922.

[33] Herholz K, Salmon E, Perani D, et al. Discrimination between Alzheimer dementia and controls by automated analysis of multicenter FDG PET. Neuroimage. Sep 2002;17(1):302-316.

[34] Smith SM, Nichols TE. Threshold-free cluster enhancement: addressing problems of smoothing, threshold dependence and localisation in cluster inference. Neuroimage. Jan 1 2009;44(1):83-98.

[35] Edison P, Archer HA, Hinz R, et al. Amyloid, hypometabolism, and cognition in Alzheimer disease: an [11C]PIB and [18F]FDG PET study. Neurology. Feb 13 2007;68(7):501-508.

[36] Koedam EL, Lehmann M, van der Flier WM, et al. Visual assessment of posterior atrophy development of a MRI rating scale. Eur Radiol. Dec 2011;21(12):2618-2625.

[37] Borroni B, Grassi M, Premi E, et al. Neuroanatomical correlates of behavioural phenotypes in behavioural variant of frontotemporal dementia. Behav Brain Res. Dec 1 2012;235(2):124-129.

[38] Ibanez V, Pietrini P, Alexander GE, et al. Regional glucose metabolic abnormalities are not

the result of atrophy in Alzheimer's disease. Neurology. Jun 1998;50(6):1585-1593.

[39] Shimizu S, Zhang Y, Laxamana J, et al. Concordance and discordance between brain perfusion and atrophy in frontotemporal dementia. Brain Imaging Behav. Mar 2010;4(1):46-54.

[40] Hutton B.F BAT, K. Erlandsson, et al. . What approach to brain partial volume correction is best for PET/MRI? Nuclear Instruments and Methods in Physics Research A. 2013(702):29-33.